ACS Catalysis

pubs.acs.org/acscatalysis

Research Article

# Linear Regression Model Development for Analysis of Asymmetric Copper-Bisoxazoline Catalysis

Jacob Werth and Matthew S. Sigman*

Cite This: *ACS Catal.* 2021, 11, 3916–3922

Read Online

ACCESS | Metrics & More | Article Recommendations | Supporting Information

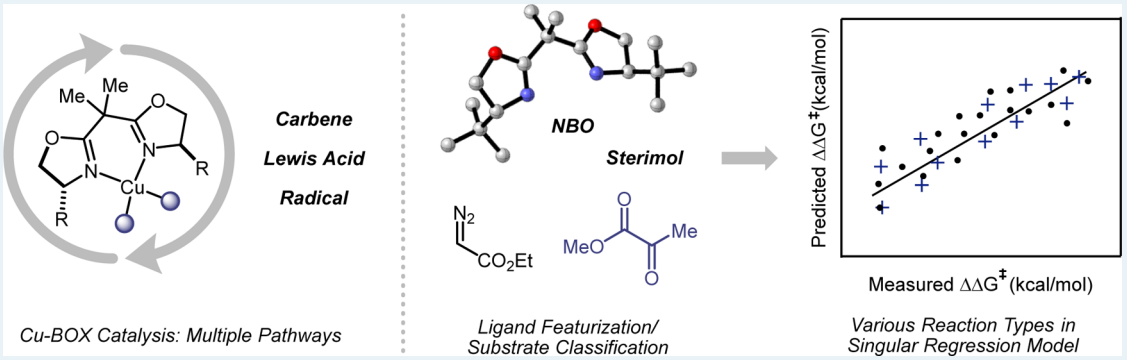


**ABSTRACT:** Multivariate linear regression (MLR) analysis is used to unify and correlate different categories of asymmetric Cu-bisoxazoline (BOX) catalysis. The versatility of Cu-BOX complexes has been leveraged for several types of enantioselective transformations including cyclopropanation, Diels–Alder cycloadditions, and difunctionalization of alkenes. Statistical tools and extensive molecular featurization have guided the development of an inclusive linear regression model, providing a predictive platform and readily interpretable descriptors. Mechanism-specific categorization of curated data sets and parameterization of reaction components allow for simultaneous analysis of disparate organometallic intermediates such as carbenes and Lewis acid adducts, all unified by a common ligand scaffold and metal ion. Additionally, this workflow permitted the development of a complementary linear regression model correlating analogous BOX-catalyzed reactions employing Ni, Fe, Mg, and Pd complexes. Comparison of ligand parameters in each model reveals the relevant structural requirements necessary for high selectivity. Overall, this strategy highlights the utility of MLR analysis in exploring mechanistically driven correlations across a diverse chemical space in organometallic chemistry and presents an applicable workflow for related ligand classes.

**KEYWORDS:** *asymmetric catalysis, copper, bisoxazoline, data science, carbene, Lewis acid, radical*



## INTRODUCTION

Bisoxazoline (BOX) ligands have been extensively used as universal bidentate ligands in asymmetric catalysis due to their readily tunable features, conformational rigidity, and ability to create highly selective environments.[1] Their ubiquity in the field has brought on decades of iterative designs, accessing coordination with numerous metal ions capable of wide-ranging bond forming processes.[2] Particularly, Cu-BOX catalysts have been employed for many types of mechanistically diverse transformations, such as cyclopropanation and Diels–Alder reactions.[3] More recently, these complexes have been applied to realize enantioselective variants of radical-based difunctionalization of alkenes and C–H functionalization.[4]

This remarkable spectrum of mechanistic processes has brought on in-depth computational studies throughout the years including transition state analysis and quadrant-based regression analysis.[5] However, the focus of these studies has been limited to one specific mechanism and/or reaction type. Our group has recently applied data science tools toward building multivariate linear regression (MLR) models for various areas of hydrogen bond donor catalysis including binol-derived chiral phosphoric acid and thiourea-based catalysts.[6] Data mining these reactions of interest has allowed us to understand the key elements required for asymmetric induction through the quantification of noncovalent interactions and can be leveraged for predictive capabilities.[7] By expanding the subject of study to multiple mechanistic pathways, we can begin to explore structural patterns beyond one reaction type. In this vein, we sought to apply this

Received: February 3, 2021
Revised: March 3, 2021
Published: March 15, 2021




https://dx.doi.org/10.1021/acscatal.1c00531
*ACS Catal.* 2021, 11, 3916–3922

workflow to a suitable class of asymmetric catalysis wherein distinct transition states are unified by a similar catalyst structure. Given the broad scope of reactivity exhibited by Cu-BOX complexes, this body of literature presented an ideal case study. Throughout the development stage of this study, many questions were posed as part of the hypothesis: (1) Considering the multiple modes of asymmetric Cu-BOX catalysis, can structural relationships between these various pathways be used to correlate enantioselectivity using a statistical model? (2) Given the limited feature overlap between the reaction coupling partners, can an adequate parameter set be built to accurately distinguish molecular structures? (3) Finally, can Cu-BOX-catalyzed reactions be correlated with other metal-BOX-catalyzed transformations? We report here the multireaction linear regression analysis of Cu-BOX-catalyzed reactions through curation of carbene, Lewis acid and radical-based transformations from the primary literature. The proposed mechanisms of these various transformations are reflected in the categorization of reaction class and grouping of substrate type, leading to meaningful connections in a singular model. As a result, mechanistic transferability is established through successful prediction of out of sample reactions (Figure 1).

**Reaction Selection.** Initially, we categorized the Cu-BOX literature into three general reaction types: carbene, Lewis acid and radical (Figure 1a) due to the defined character of the proposed transition states. As mentioned previously, the substrates are quite disparate, which limits the complexity of parameters that can be deployed. Our hypothesis was that the consistency of the ligand structures would provide the framework to connect the transformations in the statistical models. Considering the various reactions and quantity of data available, ligand screening panels were the main focus of data curation to (1) gain insight into the catalyst structure and the essentials for selectivity and (2) limit the diversity of reaction components.

A total of 68 reactions (extracted from 10 publications) were curated for statistical modeling, spanning a selectivity window of 0−99% ee (0.0−3.1 kcal/mol).[3b,5a,8] An approximate total of 79 BOX ligands including derivatives such as AzaBOX (nitrogen bridge),[8d] IndaBOX (indane-derived),[9] SaBOX (side-arm modification),[10] TOX (trisoxazoline),[10] and the recently developed sBOX (serine-derived)[8c] were used in the analysis comprising training set data and external test sets (Figure 2). An overview of the computational workflow is highlighted in Figure 1b. Initial attempts of unconstrained conformational searches (mixed torsional/low-mode sampling) followed by density functional theory (DFT) optimization using free ligands failed due to catalytically irrelevant structures being lowest in energy. To capture the ligand framework in the context of catalysis, $CuCl_2$ was used for complexation and removed after DFT optimization (B3LYPD3BJ/6-31(d,p)/LANL2DZ(Cu)). Single point calculations were conducted on the lowest-energy ligand structure to obtain parameters of interest (M06-2X/def2-TZVP). The parameters derived from DFT calculations included Sterimol (steric descriptor), highest occupied molecular orbital (HOMO)/lowest unoccupied molecular orbital (LUMO) energies, natural bond orbital (NBO) charges, bond angles, and molecular surface area (MSA).[11] Average values for all NBO and Sterimol ligand parameters were used to describe any asymmetry between the two bisoxazoline rings and their surrounding environments.

One significant challenge in the early stages of development was determining how to group various substrates together as most of the reactions feature multiple coupling partners occupying a broad spectrum of chemical space. Guided by the proposed intermediates in the respective reactions, substrates directly bound to the Cu-center were used for comparison (Figure 3a). Unfortunately, the limited structural commonality among the substrates posed another difficulty in building a representative feature library with substrate-specific descrip-

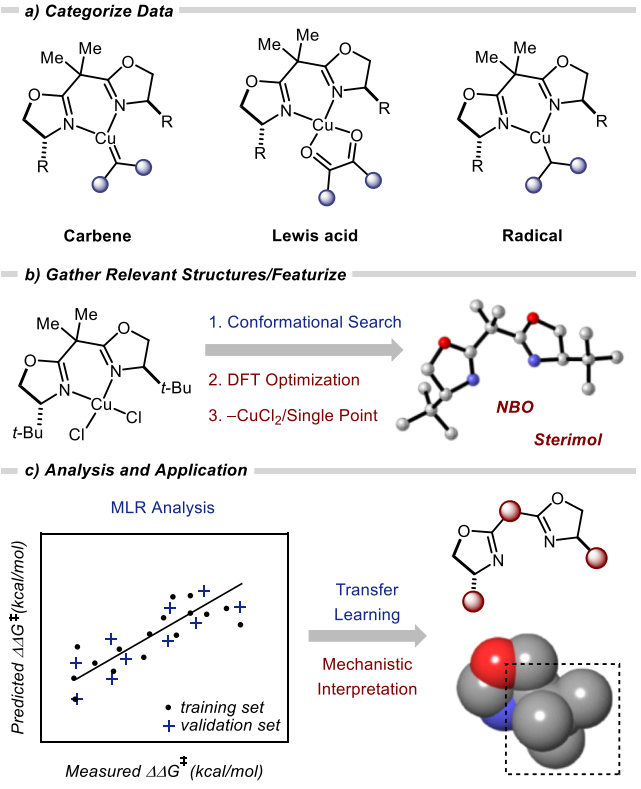


**Figure 1.** (a) Categorization of general Cu-BOX reaction intermediates invoking carbene, Lewis acid and radical-based mechanisms. (b) Workflow for computational featurization of BOX ligands. (c) MLR workflow and subsequent application toward out-of-sample predictions and mechanistic interpretation.

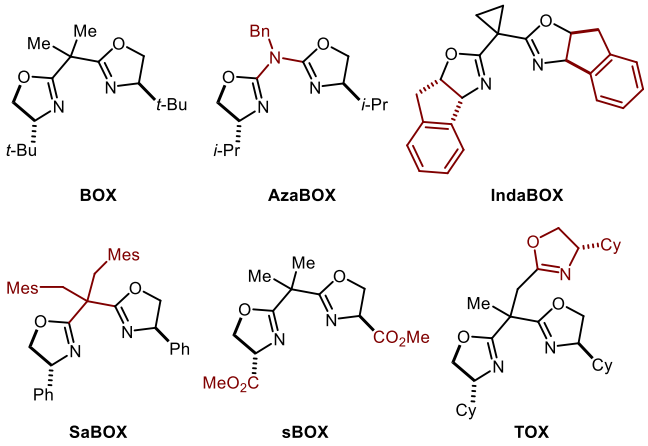


**Figure 2.** Structures of BOX derivatives used in both training sets and test sets (Mes = mesityl). Specific derivative modification highlighted in red.



https://dx.doi.org/10.1021/acscatal.1c00531
ACS Catal. 2021, 11, 3916−3922

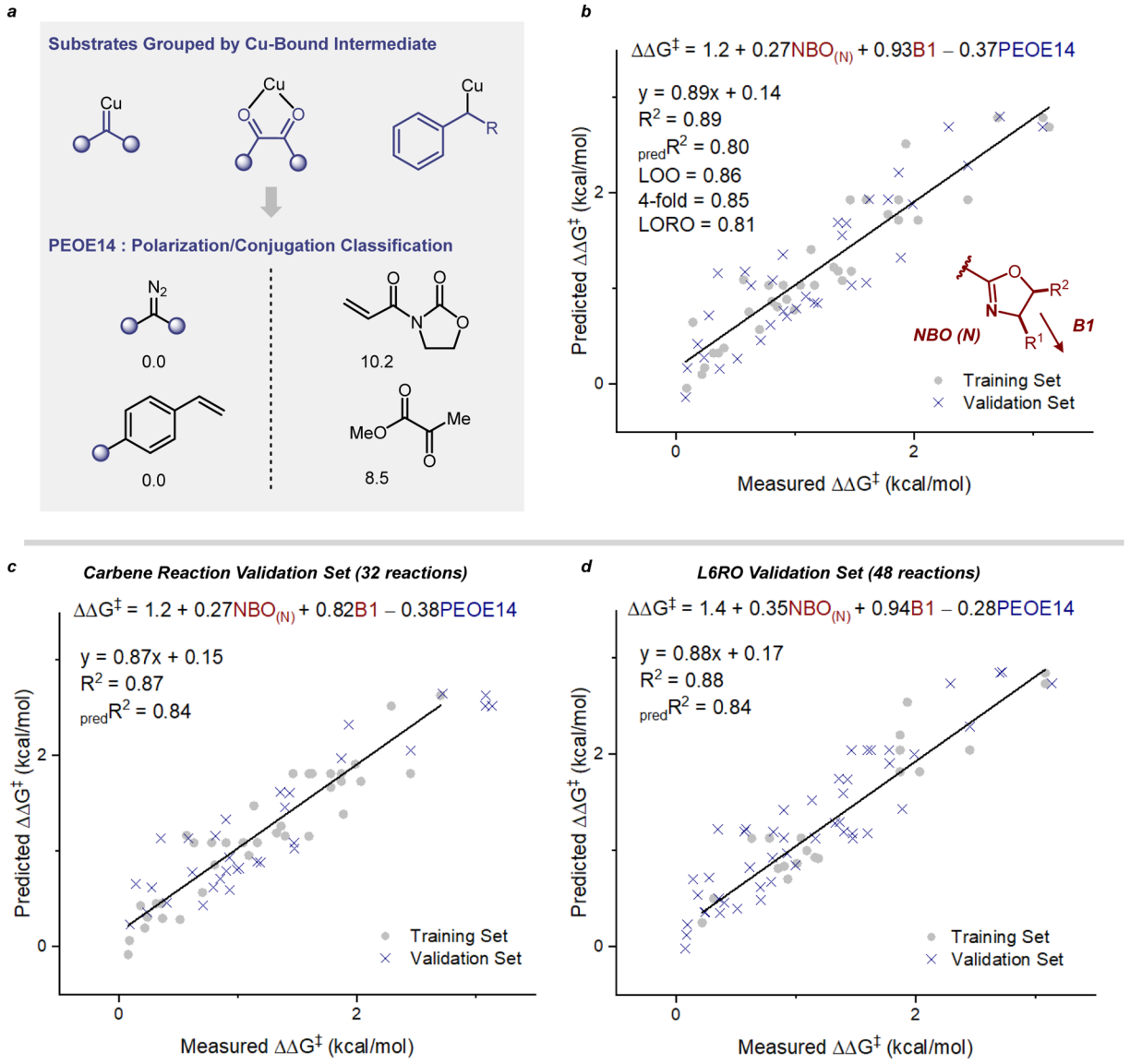


**Figure 3.** (a) Grouping of substrates based on proposed intermediates and subsequent classification using PEOE14 descriptor. (b) Multivariate regression analysis of Cu-BOX-catalyzed reactions (68 reactions). Plot of cross-validation [LOO and *k*-fold ($k = 4$)] and external validation ($_{pred}R^2$) by pseudorandom 50:50 partitioning of data into training set: validation set. (c) Plot of carbene-based reactions (32 reactions) being removed and held as a validation set. (d) Plot of six individual publications being removed (48 total reactions) and held as a validation set (L6RO = leave six reactions out).

tors. To address this limitation, molecular two-dimensional parameters typically employed for QSAR modeling were collected in addition to global DFT properties (HOMO/LUMO, polarizability, etc.).[12] This combined approach would ensure that a comprehensive parameter set could be readily assembled at a low computational cost. By focusing the training set on ligand screening data, we postulated the substrate identity could be potentially classified using simple chemical properties.

**Model Development.** Linear regression analysis was performed on the data set using the collected DFT parameters to identify potential correlations.[13] Measured enantioselectivity was calculated using Gibbs free energy equation ($\Delta\Delta G^{\ddagger} = -RT\ln|er|$) where $T$ represents the temperature of the reaction, $R$ is the gas constant, and er is the enantiomeric ratio. This allows for the screening data that employed various temperatures to be incorporated into the training set. Absolute enantiomeric excesses were used in the modeling process to ensure an evenly distributed data set and eliminate potential bias. This approach allows for inclusive retrospective analysis, obviating the requirement for absolute configuration assignment in data collection. Forward stepwise linear regression was used to identify model candidates which were evaluated based on common statistical metrics [$R^2$, leave-one-out (LOO), *k*-fold] as well as more qualitative metrics such as minimal number of parameters and the presence of cross-terms.

Throughout the model selection process, NBO(N) and Sterimol B1 ligand descriptors were consistently found imperative. A good correlation was found for the data set ($R^2 = 0.89$) using only three parameters (Figure 3b). The partial equalization of orbital electronegativity (PEOE)-14 term greatly improved the models generated through forward stepwise linear regression and was identified as the optimal parameter in distinguishing substrate structure.[14] The


https://dx.doi.org/10.1021/acscatal.1c00531
ACS Catal. 2021, 11, 3916−3922

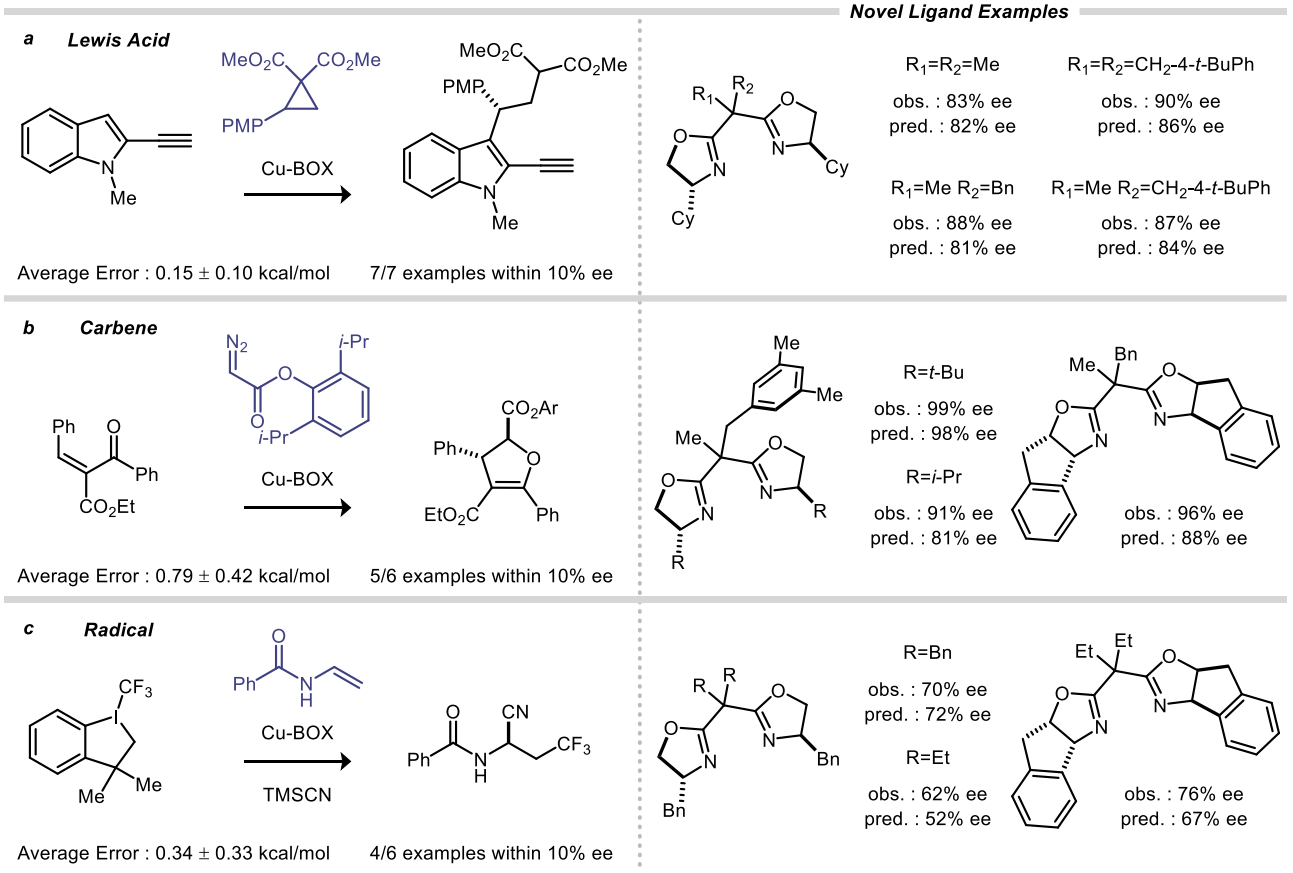


**Figure 4.** Model prediction of external test sets. Substrates highlighted in blue were used for PEOE14 calculation based upon the proposed reaction intermediates. (a) Lewis acid-mediated cyclopropane ring-opening/addition to indoles (6 novel ligands). (b) Diazo-based [4 + 1] cycloaddition (6 novel ligands). (c) Radical-based cyanation/trifluoromethylation of enamides (4 novel ligands). Novel ligand examples for each reaction highlight the prediction strength of the model (obs. = observed, pred. = predicted).

descriptor ranks substrates based upon the electronegativity of atoms as well as the overall degree of conjugation. Interestingly, this classification generally divides the substrates into two categories: carbene/radical-based substrates and Lewis acid-based substrates. Parameters encapsulating solvent/additive effects as well as reaction concentration and catalyst loading were found ineffective in achieving an improved correlation.

Cross-validation analysis and external validation were used to indicate a robust model (LOO = 0.86, 4-fold = 0.85, $_{pred}R^2$ = 0.80). External validation was completed by pseudorandom partitioning of the entire data set into 50:50, training set: validation set. Leave-one-reaction-out (LORO) analysis was used to test the general predictive capability by removing one reaction (determined by individual publications) and designating it as a validation set. The model is retrained on the remaining data and deployed for prediction of the left-out reaction. Remarkably, a LORO average of $_{pred}R^2 = 0.81 \pm 0.13$ was achieved for all 10 publications.

With the positive results from statistical validation in hand, the model was additionally tested by removing all carbene reactions (32 reactions) from the training set and held as a validation set (Figure 3c). The remaining data points were carried through as the training set with forward stepwise linear regression. Interestingly, the same 3-parameter model (NBO(N), B1, PEOE14) was found optimal. A high $_{pred}R^2$ score (0.84) indicated that the model was not dependent on one mechanistic type and could accurately predict new mechanism types. To further challenge the model, 6 out of the 10 publications were removed (48 reactions) and held as a validation set (Figure 3d). The remaining data set (20 reactions) consisted of all three mechanistic types and was once again submitted to a forward step linear regression as the new training set. Due to the size constraint of the training set, it was necessary to include at least one example from each reaction category. Notably, the global model was still found to be the optimal 3-parameter model and a high $_{pred}R^2$ score of 0.84 was calculated further supporting the robust nature of the model. This validation was repeated in the same manner using four different publications as the training set (27 reactions) and similar results were obtained (see the Supporting Information for details).

**Prediction of New Reaction Types.** The next step in our workflow assessed the predictive capability of our model toward external ligand screening data sets (Figure 4). These case studies were selected to specifically challenge the model's ability to predict novel ligands/substrates as well as unique reactivity not captured in the training set. All test cases below include new ligands (as noted) and substrates. Assessment of the predictive capability was conducted using average absolute prediction error (kcal/mol) and the number of examples falling within 10% ee error. This extensive analysis provides multiple outputs for evaluation, especially considering the logarithmic function of $\Delta\Delta G^{\ddagger}$.


https://dx.doi.org/10.1021/acscatal.1c00531
ACS Catal. 2021, 11, 3916−3922

As a first scenario, a Lewis acid-mediated cyclopropane ring-opening/addition to indoles was predicted (Figure 4a).[15] This test set included 6 new ligand structures, all including cyclohexyl substitution of the bisoxazoline ring, which is not represented in the training set.

Furthermore, the cyclopropane substrate proposed to form a Lewis acid adduct with the Cu catalyst is novel to the training set and represents a PEOE14 score of 0.0, contrasting to most Lewis acid-based substrates in the training set. The average prediction error was calculated to be quite low (0.15 ± 0.10 kcal/mol) with all 7 examples falling within 10% ee and 5/7 examples within 5% ee. This example highlights the model's ability to extrapolate to novel ligand substitution and reactivity, indicative of its practicality in future reaction development.

The second test was a diazo-based [4 + 1] cycloaddition (Figure 4b).[16] This reaction included 6 novel ligands with the majority of the structural variation of the ligand architecture occurring on the methylene bridge. This is an interesting scenario as all reactions featuring diazo-based substrates in the training set result in cyclopropane products. The average prediction error was found to be relatively high (0.79 ± 0.42 kcal/mol); however, these reactions generally had higher overall observed enantioselectivity and 5/6 examples were predicted within 10% ee. Of particular note is the model's capability to predict the best performing ligand within 1% ee.

Finally, a novel radical-based cyanation/trifluoromethylation of enamides reported by Liu et al. could be predicted with a low overall error (0.34 ± 0.33 kcal/mol) as shown in Figure 4c.[17] Four novel ligand structures were included in this test set, all of which were predicted within 10% ee. Collectively, these prediction case studies validate the mechanistic transferability of the model to new reaction types as shown by the low prediction error.

**Model Interpretation.** The simplicity of the linear regression model encouraged us to further explore the role of each descriptor. The largest parameter coefficient belongs to the Sterimol B1 term and its positive value indicated the presence of a general trend correlating higher enantioselectivity with larger B1 values. Upon closer inspection, a partition at approximately 85% ee can be plotted using B1 = 2.05 as an intermediate value (Figure 5). Moreover, this trend is consistent across iterations of ligand design such as sBOX (cyanation of vinylarenes) and traditional BOX (cyclopropanation of styrene), which target different reactivity.

Although a clear relationship between the Sterimol B1 parameter and selectivity was observed, the NBO(N) descriptor could not be similarly deconstructed. Considering only two ligand parameters were necessary for a comprehensive model, we further explored the subtle role this parameter has in differentiating ligand classes.

A qualitative evaluation of the ligands revealed a connection between larger ring sizes featured on the bridge atom and lower NBO(N) values, suggesting that this substitution may be an influence (Figure 6a). Linear regression analysis of NBO(N) as an output (in lieu of $\Delta\Delta G^{\ddagger}$) was employed to further define the parameter and revealed a suitable three-term model composed of non-collinear ligand parameters (Figure 6b).

Univariate analysis of the NBO(C=N) component indicated a classification of BOX versus AzaBOX ligands due to the proximity of the nitrogen to the bridge atom. Furthermore, MSA(bridge) of the free ligand and bite angle ($\theta$) of the Cu-bound complex were critical for correlation. The bite angle of the metal complex has been shown to trend with selectivity in discrete data sets.[18] Together, these two parameters provide a general description of the bridge atom substitution and their presence in the model suggests that the NBO(N) term is expressing a distal influence. Using linear regression analysis to study individual parameters in this manner demonstrates the sophistication of these descriptors and how much chemical information they imbed.

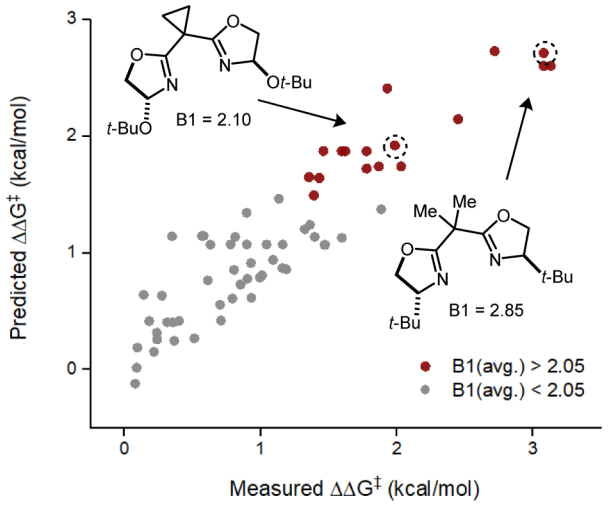


**Figure 5.** Linear regression plot highlighting the general benefit of larger Sterimol B1 values on enantioselectivity. Specific examples include enantioselective cyclopropanation (Evans) and cyanofunctionalization (Lin).

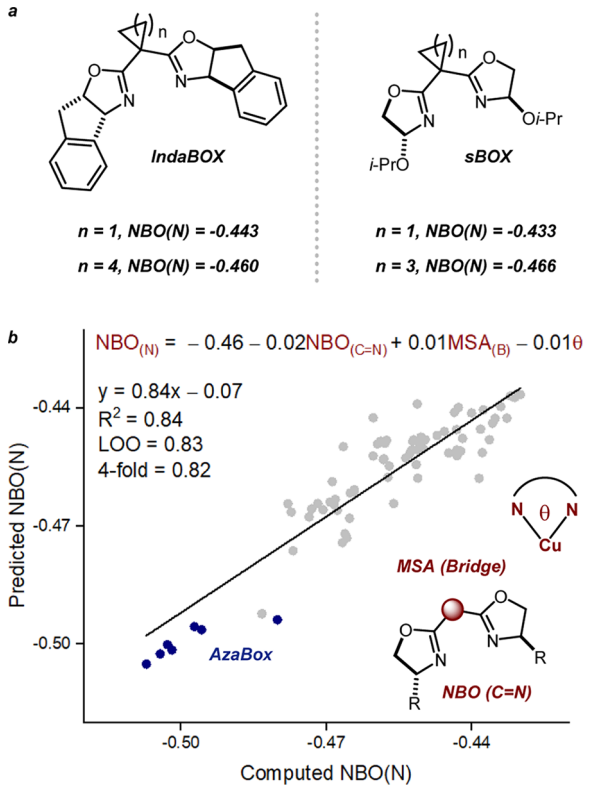


**Figure 6.** (a) Examples of IndaBOX and sBOX ligands highlighting the relationship between the chemical environment of the methylene bridge and NBO(N) descriptor. (b) Linear regression plot of NBO(N) using ligand/catalyst parameters (79 ligands).


https://dx.doi.org/10.1021/acscatal.1c00531
ACS Catal. 2021, 11, 3916−3922

**Extension to Analogous M-BOX-Catalyzed Systems.** In an attempt to expand beyond Cu-based systems, other data sets were curated featuring Fe, Ni, Mg, and Pd-BOX-catalyzed reactions. The reactivity profiles of these transformations are quite dissimilar in comparison to the three categories of Cu-BOX catalysis highlighted above including the activation of oxaziridines (Fe),[19] reductive cross-coupling (Ni),[20] and allylic alkylation (Pd).[21] Initial modeling efforts indicated that these classes of reactions would not correlate well with the Cu-based training set. Additionally, computing and collecting ligand parameters derived from the metal of interest did not significantly improve statistics. Surprisingly, we discovered these reactions could be successfully modeled as a separate data set (24 reactions) as depicted in Figure 7.[19−22] Forward

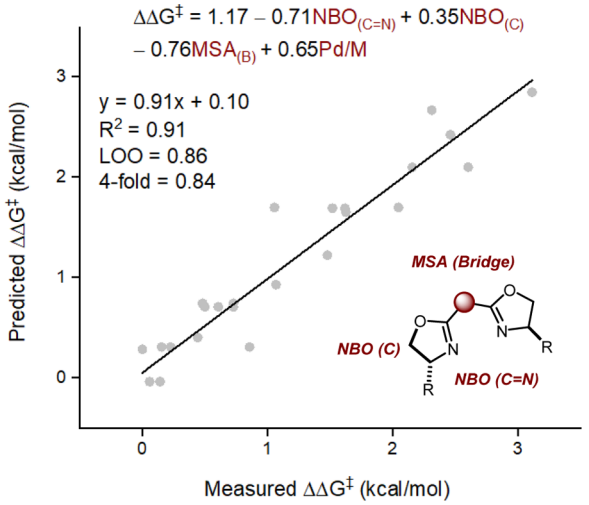


**Figure 7.** MLR plot of Fe/Ni/Mg/Pd-BOX-catalyzed reactions.

stepwise linear regression yielded a statistically robust model ($R^2$ = 0.91, LOO = 0.86, 4-fold = 0.84) using three ligand-based parameters and a classifier for Pd-catalyzed reactions. Although topological-based parameters were found useful for correlation, it was discovered a simple binary classification (Pd/M) for differentiating Pd (1) from other metals (0) provided the optimal model.

Assessment of the parameters explains the failed attempt to correlate these reactions with the Cu-based training set. Interestingly, the model shares two common parameters with the linear regression output of NBO(N). However, the relative magnitudes of common parameters are quite different between the two models suggesting that the descriptors are playing unique roles in correlating with enantioselectivity. Upon closer inspection, the M-BOX-catalyzed reactions greatly depend on the steric/electronic environment of the methylene bridge. In contrast, the Cu-BOX model does not require an explicit parameter describing the bridge of the ligand and critically depends on the steric discrimination of the bisoxazoline ring. Furthermore, the reactivity between these two systems may be significantly influenced by the saturation of coordination sites specific to the identity of the metal.

## CONCLUSIONS

In summary, a retrospective survey of Cu-BOX-catalyzed enantioselective reactions has provided a data science-driven model correlating various reaction pathways including carbene, Lewis acid and radical-based Cu-intermediates. Our workflow allows for the simultaneous study of unique transition states by featurizing common chemical space through similar metal/ligand combinations. Categorization of the proposed intermediates and a simple classification of reaction partners enable robust model development allowing for prediction of new reaction types and novel ligand structures. Furthermore, deconstruction of the parameters unveils a sterically driven trend of selectivity and an NBO charge capable of describing subtle structural changes. As the development of statistical toolsets progresses, underlying connections between reaction classes can be discovered, revealing general mechanistic principles. This is an ongoing goal of our research program.

## ASSOCIATED CONTENT

### Supporting Information

The Supporting Information is available free of charge at https://pubs.acs.org/doi/10.1021/acscatal.1c00531.

BOX/substrate parameters (XLSX)
Computational methods and details (PDF)

## AUTHOR INFORMATION

### Corresponding Author

**Matthew S. Sigman** − *Department of Chemistry, University of Utah, Salt Lake City, Utah 84112, United States;* orcid.org/0000-0002-5746-8830; Email: matt.sigman@utah.edu

### Author

**Jacob Werth** − *Department of Chemistry, University of Utah, Salt Lake City, Utah 84112, United States;* orcid.org/0000-0001-9648-5986

Complete contact information is available at: https://pubs.acs.org/10.1021/acscatal.1c00531

### Notes

The authors declare no competing financial interest.

## ACKNOWLEDGMENTS

This research was supported by the NIH (R35 GM136271).

## REFERENCES

(1) Yoon, T. P.; Jacobsen, E. N. Privileged Chiral Catalysts. *Science* **2003**, *299*, 1691.

(2) (a) Desimoni, G.; Faita, G.; Jørgensen, K. A. C2-Symmetric Chiral Bis(Oxazoline) Ligands in Asymmetric Catalysis. *Chem. Rev.* **2006**, *106*, 3561−3651. (b) Desimoni, G.; Faita, G.; Jørgensen, K. A. Update 1 of: C2-Symmetric Chiral Bis(oxazoline) Ligands in Asymmetric Catalysis. *Chem. Rev.* **2011**, *111*, PR284−PR437.

(3) (a) Johnson, J. S.; Evans, D. A. Chiral Bis(oxazoline) Copper(II) Complexes: Versatile Catalysts for Enantioselective Cycloaddition, Aldol, Michael, and Carbonyl Ene Reactions. *Acc. Chem. Res.* **2000**, *33*, 325−335. (b) Evans, D. A.; Woerpel, K. A.; Hinman, M. M.; Faul, M. M. Bis(oxazolines) as chiral ligands in metal-catalyzed asymmetric reactions. Catalytic, asymmetric cyclopropanation of olefins. *J. Am. Chem. Soc.* **1991**, *113*, 726−728.

(4) (a) Li, Z.-L.; Fang, G.-C.; Gu, Q.-S.; Liu, X.-Y. Recent advances in copper-catalysed radical-involved asymmetric 1,2-difunctionalization of alkenes. *Chem. Soc. Rev.* **2020**, *49*, 32−48. (b) Zhang, W.; Wang, F.; McCann, S. D.; Wang, D.; Chen, P.; Stahl, S. S.; Liu, G. Enantioselective cyanation of benzylic C−H bonds via copper-catalyzed radical relay. *Science* **2016**, *353*, 1014.

(5) (a) Aguado-Ullate, S.; Urbano-Cuadrado, M.; Villalba, I.; Pires, E.; García, J. I.; Bo, C.; Carbó, J. J. Predicting the Enantioselectivity of the Copper-Catalysed Cyclopropanation of Alkenes by Using

Quantitative Quadrant-Diagram Representations of the Catalysts. *Chem.—Eur. J.* **2012**, *18*, 14026−14036. (b) Lipkowitz, K. B.; Pradhan, M. Computational Studies of Chiral Catalysts: A Comparative Molecular Field Analysis of an Asymmetric Diels−Alder Reaction with Catalysts Containing Bisoxazoline or Phosphinooxazoline Ligands. *J. Org. Chem.* **2003**, *68*, 4648−4656. (c) Rasmussen, T.; Jensen, J. F.; Østergaard, N.; Tanner, D.; Ziegler, T.; Norrby, P.-O. On the Mechanism of the Copper-Catalyzed Cyclopropanation Reaction. *Chem.—Eur. J.* **2002**, *8*, 177−184. (d) Deeth, R. J.; Fey, N. A Molecular Mechanics Study of Copper(II)-Catalyzed Asymmetric Diels−Alder Reactions. *Organometallics* **2004**, *23*, 1042−1054.

(6) (a) Werth, J.; Sigman, M. S. Connecting and Analyzing Enantioselective Bifunctional Hydrogen Bond Donor Catalysis Using Data Science Tools. *J. Am. Chem. Soc.* **2020**, *142*, 16382−16391. (b) Reid, J. P.; Sigman, M. S. Holistic prediction of enantioselectivity in asymmetric catalysis. *Nature* **2019**, *571*, 343−348.

(7) (a) Knowles, R. R.; Jacobsen, E. N. Attractive noncovalent interactions in asymmetric catalysis: Links between enzymes and small molecule catalysts. *Proc. Natl. Acad. Sci. U.S.A.* **2010**, *107*, 20678. (b) Reid, J. P.; Sigman, M. S. Comparing quantitative prediction methods for the discovery of small-molecule chiral catalysts. *Nat. Rev. Chem.* **2018**, *2*, 290−305.

(8) (a) Evans, D. A.; Burgey, C. S.; Kozlowski, M. C.; Tregay, S. W. C2-Symmetric Copper(II) Complexes as Chiral Lewis Acids. Scope and Mechanism of the Catalytic Enantioselective Aldol Additions of Enolsilanes to Pyruvate Esters. *J. Am. Chem. Soc.* **1999**, *121*, 686−699. (b) Evans, D. A.; Miller, S. J.; Lectka, T.; von Matt, P. Chiral Bis(oxazoline)copper(II) Complexes as Lewis Acid Catalysts for the Enantioselective Diels−Alder Reaction. *J. Am. Chem. Soc.* **1999**, *121*, 7559−7573. (c) Fu, N.; Song, L.; Liu, J.; Shen, Y.; Siu, J. C.; Lin, S. New Bisoxazoline Ligands Enable Enantioselective Electrocatalytic Cyanofunctionalization of Vinylarenes. *J. Am. Chem. Soc.* **2019**, *141*, 14480−14485. (d) Glos, M.; Reiser, O. Aza-bis(oxazolines): New Chiral Ligands for Asymmetric Catalysis. *Org. Lett.* **2000**, *2*, 2045−2048. (e) Itagaki, M.; Yamamoto, Y. Application of a chiral copper-1,1-bis{2-[(4S)-*tert*-butyloxazolinyl]}cyclopropane catalyst for asymmetric cyclopropanation of styrene. *Tetrahedron Lett.* **2006**, *47*, 523−525. (f) Palomo, C.; Oiarbide, M.; Halder, R.; Kelso, M.; Gómez-Bengoa, E.; García, J. M. Catalytic Enantioselective Conjugate Addition of Carbamates. *J. Am. Chem. Soc.* **2004**, *126*, 9188−9189. (g) Yao, S.; Johannsen, M.; Audrain, H.; Hazell, R. G.; Jørgensen, K. A. Catalytic Asymmetric Hetero-Diels−Alder Reactions of Ketones: Chemzymatic Reactions. *J. Am. Chem. Soc.* **1998**, *120*, 8599−8605. (h) Zhang, G.; Fu, L.; Chen, P.; Zou, J.; Liu, G. Proton-Coupled Electron Transfer Enables Tandem Radical Relay for Asymmetric Copper-Catalyzed Phosphinoylcyanation of Styrenes. *Org. Lett.* **2019**, *21*, 5015−5020.

(9) Davies, I. W.; Senanayake, C. H.; Larsen, R. D.; Verhoeven, T. R.; Reider, P. J. Application of a Ritter-type reaction to the synthesis of chiral indane-derived C2-symmetric bis(oxazolines). *Tetrahedron Lett.* **1996**, *37*, 813−814.

(10) Liao, S.; Sun, X.-L.; Tang, Y. Side Arm Strategy for Catalyst Design: Modifying Bisoxazolines for Remote Control of Enantioselection and Related. *Acc. Chem. Res.* **2014**, *47*, 2260−2272.

(11) Santiago, C. B.; Guo, J.-Y.; Sigman, M. S. Predictive and mechanistic multivariate linear regression models for reaction development. *Chem. Sci.* **2018**, *9*, 2398−2412.

(12) (a) Cherkasov, A.; Muratov, E. N.; Fourches, D.; Varnek, A.; Baskin, I. I.; Cronin, M.; Dearden, J.; Gramatica, P.; Martin, Y. C.; Todeschini, R.; Consonni, V.; Kuz'min, V. E.; Cramer, R.; Benigni, R.; Yang, C.; Rathman, J.; Terfloth, L.; Gasteiger, J.; Richard, A.; Tropsha, A. QSAR Modeling: Where Have You Been? Where Are You Going To? *J. Med. Chem.* **2014**, *57*, 4977−5010. (b) Hansch, C.; Leo, A. *Exploring QSAR: Fundamentals and Applications in Chemistry and Biology*; ACS, 1995.

(13) Guo, J.-Y.; Minko, Y.; Santiago, C. B.; Sigman, M. S. Developing Comprehensive Computational Parameter Sets To Describe the Performance of Pyridine-Oxazoline and Related Ligands. *ACS Catal.* **2017**, *7*, 4144−4151.

(14) Gasteiger, J.; Marsili, M. Iterative partial equalization of orbital electronegativity—a rapid access to atomic charges. *Tetrahedron* **1980**, *36*, 3219−3228.

(15) Liu, Q.-J.; Yan, W.-G.; Wang, L.; Zhang, X. P.; Tang, Y. One-Pot Catalytic Asymmetric Synthesis of Tetrahydrocarbazoles. *Org. Lett.* **2015**, *17*, 4014−4017.

(16) Zhou, J.-L.; Wang, L.-J.; Xu, H.; Sun, X.-L.; Tang, Y. Highly Enantioselective Synthesis of Multifunctionalized Dihydrofurans by Copper-Catalyzed Asymmetric [4 + 1] Cycloadditions of $\alpha$-Benzylidene-$\beta$-ketoester with Diazo Compound. *ACS Catal.* **2013**, *3*, 685−688.

(17) Zhang, G.; Zhou, S.; Fu, L.; Chen, P.; Li, Y.; Zou, J.; Liu, G. Asymmetric Coupling of Carbon-Centered Radicals Adjacent to Nitrogen: Copper-Catalyzed Cyanation and Etherification of Enamides. *Angew. Chem., Int. Ed.* **2020**, *59*, 20439−20444.

(18) Davies, I. W.; Deeth, R. J.; Larsen, R. D.; Reider, P. J. A CLFSE/MM study on the role of ligand bite-angle in Cu(II)-catalyzed Diels-Alder reactions. *Tetrahedron Lett.* **1999**, *40*, 1233−1236.

(19) Williamson, K. S.; Yoon, T. P. Iron Catalyzed Asymmetric Oxyamination of Olefins. *J. Am. Chem. Soc.* **2012**, *134*, 12370−12373.

(20) Hofstra, J. L.; Cherney, A. H.; Ordner, C. M.; Reisman, S. E. Synthesis of Enantioenriched Allylic Silanes via Nickel-Catalyzed Reductive Cross-Coupling. *J. Am. Chem. Soc.* **2018**, *140*, 139−142.

(21) Matt, P. V.; Lloyd-Jones, G. C.; Minidis, A. B. E.; Pfaltz, A.; Macko, L.; Neuburger, M.; Zehnder, M.; Rüegger, H.; Pregosin, P. S. Enantioselective Allylic Substitution Catalyzed by Chiral [Bis-(dihydrooxazole)]palladium Complexes: Catalyst structure and possible mechanism of enantioselection. *Helv. Chim. Acta* **1995**, *78*, 265−284.

(22) (a) Gottumukkala, A. L.; Matcha, K.; Lutz, M.; de Vries, J. G.; Minnaard, A. J. Palladium-Catalyzed Asymmetric Quaternary Stereocenter Formation. *Chem.—Eur. J.* **2012**, *18*, 6907−6914. (b) Sibi, M. P.; Itoh, K.; Jasperse, C. P. Chiral Lewis Acid Catalysis in Nitrile Oxide Cycloadditions. *J. Am. Chem. Soc.* **2004**, *126*, 5366−5367.



https://dx.doi.org/10.1021/acscatal.1c00531
*ACS Catal.* 2021, 11, 3916−3922